Electroabsorption spectroscopy: A versatile tool to measure optical nonlinearities

W. D. R. Joseph, N. R. Pradhan, Suneel Singh and D. Narayana Rao*

School of Physics, University of Hyderabad, Hyderabad 500 046, India

Electroabsorption spectra are recorded at room temperature for free-base hydrogen tetratolylporphyrin (H_2TTP) dispersed in poly (methyl methacrylate) polymer. The electroabsorption spectrum of H_2TTP recorded at the second harmonic (2Ω) of the applied electric field frequency Ω, has a line shape that resembles the mathematical first derivative of the linear absorption spectrum. The observed line-shape is as expected for electric field dependence of change in polarizability contribution to electroabsorption. The third-order nonlinear susceptibility $\chi^{(3)}$ leading to the second hyperpolarizability $\langle\gamma\rangle$ of H_2TTP is estimated to be 0.388×10^{-30} esu at 532 nm, which is comparable with that measured through degenerate four-wave mixing technique.

STARK spectroscopy or electroabsorption spectroscopy is the study of the effect of an applied electric field on the characteristic light absorption (or emission) spectrum of a material. This technique has been used to probe the electronic structure of varied materials and from gas-phase molecules to band structure of semiconductors[1–8]. Though the ground-state dipole moments of many molecules (in solution state) could be realized with the help of stark spectroscopy over the years, the dipole moment and polarizability changes between ground and excited states could not be measured unambiguously. This has been overcome by immobilizing the samples in a polymer matrix or frozen glass, which also enabled the application of large fields thus making possible more precise investigation into electro-optical properties. Boxer and co-workers have made pioneering contributions to the stark spectroscopy of electronic transitions in a variety of molecular materials as well as chemical and biological systems[9]. There are other exotic electroabsorption studies on varied materials such as π-conjugated polymers probing polymer disorder[10] and on molecular inorganic materials by Hupp and co-workers[11].

Porphyrins have properties suitable for opto-electronic applications[12,13]. They have greater thermal stability in comparison to organic chromophores; their extended π-conjugated macro-cyclic ring makes interesting and large second- and third-order NLO effects possible; their physical properties can be engineered through chemical modification of their periphery. Porphyrins and metalloporphyrins as field-responsive materials have found broad applications in the field of opto-electronics. One can extract desired molecular and material properties such as dipole moments, polarizabilities and hyperpolarizabilities. Enhanced optical limiting properties of various appended porphyrins has been observed and has attracted much attention for their applications in solid-state sensors and for human eye protection from high-intensity, visible, light sources[14]. Anderson and co-workers have employed electroabsorption spectroscopy to explore the third-order nonlinear susceptibility of butadiene-linked porphyrin–polymer and have found good correspondence with *Z*-scan and four-wave mixing (FWM) experiments[15]. The free-base hydrogen tetratolylporphyrin (H_2TTP) had been chosen by us since it has been investigated in our laboratory for its nonlinear optical properties using conventional techniques and hence it would be an ideal molecule to demonstrate the uniqueness and usefulness of stark spectroscopy measurements in supplementing/complementing previously obtained results.

Experimental method

A tungsten–halogen lamp hosted in a home-built air-cooled housing is used as the lamp source for the visible-near-IR region. The light from the lamp is focused onto the entry aperture of a 1/4 m grating monochromator. The full width at half maximum of the individual colours exiting the monochromator is within 3 nm across the entire scan range of 380 to 750 nm. The unpolarized probe beam falls perpendicular to the sample. Light exiting the sample is then collected and focused onto a fast photodiode (FND 100) connected to a pre-amplifier (SR 552 with a gain of 100) prior to being lock-in (SR 830) detected. The sensitivity and time constant of the lock-in are carefully chosen so as to provide an averaged and stable output signal. The output of the lock-in amplifier is then fed to an ADC card in a PC. A chopper (chopping at ~ 220 Hz) placed at the exit of the monochromator is fed as reference input to the lock-in amplifier to enable recording of the linear absorption spectrum of the sample. The absorption spectrum of the sample is obtained by digitizing the transmission through the sample with respect to the empty sample cell. Semi-transparent indium tin oxide (ITO)-coated glass slides are used as electrodes. The ITO coating is etched so as to have patterned electrodes. The schematic of the experimental set-up is shown in Figure 1.

*For correspondence. (e-mail: dnrsp@uohyd.ernet.in)

The H_2TTP is a kind gift from Bhaskar G. Maiya, School of Chemistry, University of Hyderabad. A suitable amount of the porphyrin is dispersed into PMMA polymer and dissolved in spectroscopic grade chloroform to obtain a 1.96 wt% solution. The amount of chloroform is adjusted to obtain a solution of suitable viscosity. After ensuring proper dispersion of the porphyrin in the polymer, the porphyrin–polymer solution is poured onto the two-patterned ITO glass slides and spun at a speed of 4000 rpm for 30 s to form a thin film. The thin film thus formed is vacuum-dried for a couple of hours in the dark to remove any trace of solution. The ITO slides are then glued to each other to form an ITO/sample/ITO sandwich, which is then subjected to 150°C for 2 h. Thin wires, through which the external electric field is to be applied, are affixed onto the ITO surfaces on each slide with the help of silver paint/glue. The thickness of the sandwiched sample, estimated using a precision gauge is 20 micron (± 3 micron). The electric field was operated at a frequency of 220 Hz with the peak-to-peak voltage being 500 V, which results in an effective field of 0.25×10^6 V/cm across the film. Sample (dielectric) breakdown hinders the application of electric field of higher strength. The required high AC electric field is generated using a high-power amplifier (TREK609A having a fixed gain of 1000) whose input is a digitally synthesized sine waveform from the lock-in amplifier (0–10 V p-p). The output of the high power amplifier is connected to the ITO electrodes.

Results and discussion

Electroabsorption spectrum can be understood as the 'field on' spectrum minus the 'field off' spectrum. The changes in the absorption spectra due to the applied field, however, are minute, of the order of 10^{-4} to 10^{-6} and to detect such minute changes, electric fields around ~ 1 MV/cm are required. The dependence of the characteristic optical absorption of a material on an externally applied electric field exposes field-dependent photophysical and photochemical processes in addition to the information that may be gained from the difference in the 'in field' and 'field free' electronic properties of the ground state and the excited state.

At a particular known wavelength, the well-known Beer–Lambert's law gives the absorption of light by a material in terms of intensity transmitted as

$$I = I_0 \, e^{-\alpha t}, \tag{1}$$

where I_0 is the incident intensity, α is the absorption coefficient and t is the thickness of the thin sample film. Electroabsorption of a material is the electric field-induced change in its absorption coefficient and is given by

$$\Delta\alpha = -\left(\frac{1}{t}\right) \times \left(\frac{\Delta \ldots}{\ldots}\right), \tag{2}$$

where ΔI is the field-induced change in the absorption intensity.

The third-order nonlinear polarization due to the quadratic dependence of absorption on the electric field may be written as[16]

$$P_{NL}^{(3)}(2\Omega + \omega) = 3\chi^{(3)}(2\Omega + \omega; \Omega, \Omega, \omega) E(\Omega) E(\Omega) E(\omega), \tag{3}$$

where ω the optical frequency and Ω the externally applied field frequency. Since the electric field frequency is much smaller (kHz and sub-kHz range) than the optical

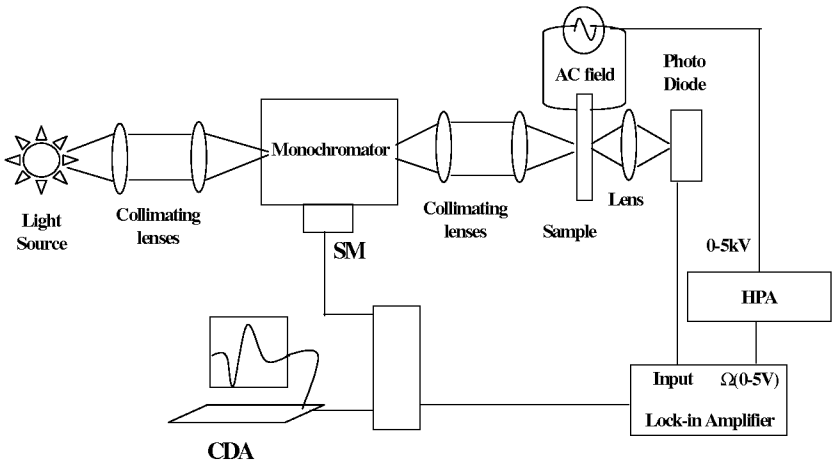

HPA – High Power Amplifier
SM – Stepper Motor
CDA – Computerized Data Acquisition

Figure 1. Experimental set-up for electroabsorption experiments.

frequency (of the order THz), one can consider the electric field frequency as a constant dc. In which case eq. (3) reduces to

$$P_{NL}^{(3)}(\omega) = 3\chi^{(3)}(\omega;0,0,\omega)\,E(\Omega)\,E(\Omega)\,E(\omega). \quad (4)$$

However, the applied field frequency is significant for the purpose of lock-in detection, as explained above. The third-order nonlinear effect represented by $\chi^{(3)}$ may be attributed to a quadratic electric field dependence of the absorption change as evident from eq. (4). Since the complex index of refraction $\hat{n} = n - ik = \sqrt{\varepsilon}$, where n and k are the real and imaginary part of the refractive index and ε is the electric permittivity of the medium, then the real and imaginary part of $\chi^{(3)}$ may be derived from the changes in refractive index in the presence of the electric field as[17]:

$$\chi_{\text{real}}^{(3)} = \left(\frac{1}{6\delta E_0^2}\right)\cdot[n(0)\cdot\Delta n - k(0)\cdot\Delta k], \quad (5)$$

$$\chi_{\text{img}}^{(3)} = \left(\frac{1}{6\delta E_0^2}\right)\cdot[n(0)\cdot\Delta k + k(0)\cdot\Delta n], \quad (6)$$

where

$$\Delta k = \frac{\lambda\Delta\alpha}{4\pi},\quad k(0) = \frac{\lambda\alpha}{4\pi},$$

$n(0)$ is the real part of refractive index, E_0 is the magnitude of the externally applied modulating electric field in V/cm and λ is the wavelength in cm. Here it must be noted that $\Delta\alpha$ as applied to eqs (5) and (6) is the change in characteristic absorption, which reflects only the second harmonic (of the field) dependence of electroabsorption. Since values of Δn and Δk are of the order of 10^{-4}, $(\Delta n)^2$, $(\Delta k)^2$ and $(\Delta n\Delta k)$ terms are omitted in eqs (5) and (6). The electric field-induced change in the refractive index Δn, may be obtained by applying a Kramers–Kronig dispersion relation[18] as:

$$\Delta n(E(\omega)) \cong \left(\frac{hc}{\delta}\right)\int_0^\infty \frac{\Delta\alpha(E(\omega'))}{[E(\omega')^2 - E(\omega)^2]}\,dE(\omega'), \quad (7)$$

where $E(\omega) = \hbar\omega$ is the energy of optical transition with frequency ω, and $\hbar$ is the Planck's constant.

In general, the externally applied electric field-induced change in absorbance, ΔA may be represented as[18]:

$$\Delta A(\omega, E_0) = \Delta A(\omega, E_0^2, 2\Omega) + \Delta A(\omega, E_0^4, 4\Omega) + \Delta A(\omega, E_0^6, 6\Omega) + \ldots. \quad (8)$$

The first, second and third terms give the quadratic, fourth and sixth power dependence of absorption on the externally applied electric field respectively. The odd power field-dependent changes in absorption vanish for an immobilized isotropic sample, as is our case.

When contribution to the electroabsorption (2Ω) spectrum is dominated by the change in polarizability alone, the line shape of the 2Ω stark spectrum follows the first derivative and the stark effect on the absorption is[19]

$$\Delta A(2\Omega,\omega) \propto \frac{\omega}{h^2c^2}\frac{\partial\left(\frac{A}{\omega}\right)}{\partial\omega}(f\Delta\hat{\alpha} : E_0^2). \quad (9)$$

Whereas when polarizability effect is negligible and the stark spectrum is governed by dipole moment changes, then

$$\Delta A(2\Omega,\omega) \propto \frac{\omega}{h^2c^2}\frac{\partial^2\left(\frac{A}{\omega}\right)}{\partial^2\omega}(f\Delta\vec{\mu}_0 E_0)^2, \quad (10)$$

where ω is a measure of the optical transition energy, h the Planck's constant, c the velocity of light, $\Delta\vec{\mu}_0$ is the difference dipole moment between the ground state and the excited state, and $\Delta\hat{\alpha}_0$ is the difference polarizability tensor between the ground state and the excited state.

Absorption and electroabsorption spectrum

The field free normalized absorption spectrum of H_2TTP dispersed in PMMA matrix recorded with electroabsorption set-up is given in Figure 2. The Soret band peak lies at 418 nm, while the four Q-band peaks lie at 511, 545, 584 and 644 nm respectively. Bublitz *et al.*[9] have discussed in detail the various effects of an externally applied electric field on the absorption profile of a molecule. The electroabsorption signal recorded with field strength of 500 V p-p at twice the applied field frequency, i.e. 440 Hz is shown in Figure 3 (indicated by triangles). The region after 530 nm is magnified 15 times to facilitate comparison. The stark spectrum overlaps with the numerical first derivative of the unperturbed absorption spectrum indicated by the hollow triangles and is magnified 100 times. Figure 3 clearly shows that the 2Ω spectrum of H_2TTP follows the first derivative, indicating a dominant contribution from the change in polarizability. That the EAS at 2Ω resembles a first derivative may also indicate that H_2TTP goes predominantly as monomer in the film. Dimers/oligomers would have led to a spectrum having higher than a first-derivative component[17]. It is also noted that the contribution of polarizability change to the stark spectrum applies not only to the Soret band but also to the Q-bands. This obviously means that all the electronic transitions of the H_2TTP respond to the electric field in the same manner with overriding contribution from polarizability changes to the observed stark spectrum. The fact that the wings and peaks of the spectrum are especially suscepti-

ble to the applied field is highlighted by the 2Ω spectrum. There is a mild kink at about 400 nm in the stark spectrum, which is also visible in the numerical first derivative of the absorption spectrum. Interestingly, the negative peak of the electroabsorption spectrum has a much lower slope when compared to the numerical first derivative line shape.

Dispersion of third-order nonlinearity and second hyperpolarizability

Here, the dispersion of the third-order susceptibility of H_2TTP/PMMA has been measured using electroabsorption spectroscopy. The stark spectrum (ΔA) recorded at the second harmonic of the applied field, that is proportional to $\Delta\alpha$, can be used to obtain the wavelength dispersion of the third-order nonlinear susceptibility, $\chi^{(3)}$ using eqs (2), (5), (6) and (7). The values of $\Delta\alpha$, are adjusted to compensate for a factor of 2 that arises due to lock-in detection at 2Ω and an additional factor of $\sqrt{2}$ is included to convert the rms output of the lock-in into peak amplitude.

$$\Delta A_{2\Omega} = \frac{2\sqrt{2}}{\ln 10}\frac{\Delta I}{I}. \tag{11}$$

Here $\chi^{(3)}$ is the effective value and not an individual component of the susceptibility tensor. Individual components of $\chi^{(3)}$ would be measurable if the incident probe beam was polarized and experiments are performed to study the angle-dependent interactions between polarization and electric field. The macroscopic third-order nonlinearity is calculated as

$$\chi^{(3)} = \sqrt{(\chi^{(3)}_{\text{real}})^2 + (\chi^{(3)}_{\text{img}})^2},$$

where the real and imaginary parts of the susceptibilities are obtained from eqs (5) and (6). The wavelength dispersion of the third-order susceptibility is plotted in Figure 4.

In order to assist in a more meaningful comparison with measurements previously done with degenerate four-wave mixing (DFWM)[20], it is necessary that the third-order nonlinearity be represented by the molecular second hyperpolarizability $\langle\gamma\rangle$, rather than the bulk susceptibility. The second hyperpolarizability of a molecule in an isotropic media is related to the third-order macroscopic susceptibility by the equation

$$\langle\gamma\rangle = \frac{\chi^{(3)}}{L^4 N}, \tag{12}$$

where

$$L = \frac{n^2+2}{3}$$

is the Lorentz local field factor, n is the linear refractive index and $N = AC$ is the number density, where A is the Avagadro number = 6.023×10^{23} and C is the concentration of the porphyrin in the polymer matrix.

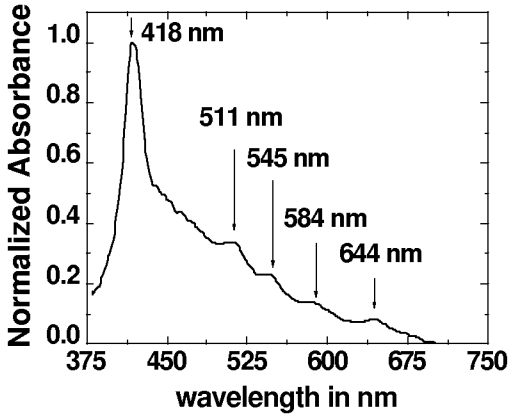

Figure 2. Absorption spectrum of H_2TTP dispersed in PMMA matrix.

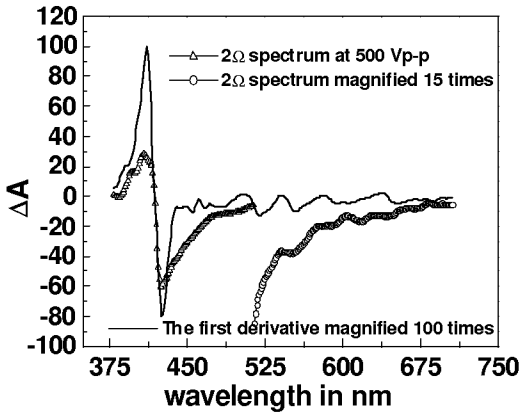

Figure 3. Electroabsorption spectrum recorded at 2Ω with field strength of 500 Vp-p is indicated by the squares. The region after 530 nm is magnified 15 times to facilitate comparison. The numerical first derivative of the absorption spectrum is also indicated by hollow triangles (magnified 100 times).

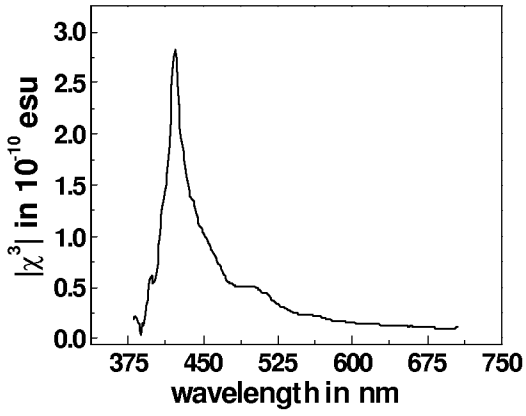

Figure 4. Dispersion of the third-order nonlinear susceptibility of H_2TTP/PMMA thin film.

The third-order susceptibility of H_2TTP from electroabsorption measurement (Figure 4) at 532 nm is $\chi^{(3)} = 29.91 \times 10^{-12}$ esu. The molecular second hyperpolarizability at 532 nm for the H_2TTP/PMMA thin film sample using electroabsorption spectroscopy obtained using eq. (12) is $(0.388 \pm 0.06) \times 10^{-30}$ esu. While nanosecond DFWM experiments performed on H_2TTP/chloroform solution resulted in $\langle\gamma\rangle = 111.40 \times 10^{-30}$ esu, the picosecond DFWM experiments gave $\langle\gamma\rangle = 1.24 \times 10^{-30}$ esu at 532 nm[21]. This large difference between the nanosecond DFWM value and electroabsorption value can be explained by the fact that the molecular second hyperpolarizability measured using the nanosecond pulses has a strong thermal contribution as well, whereas with the shorter picosecond pulses the contribution is predominantly electronic[20–22]. Picosecond DFWM (532 nm) studies performed by Maloney *et al.*[22] on free-base hydrogen tetraphenylporphyrin, which is similar to the H_2TTP we have studied, has resulted in $\chi^{(3)} = 27.93 \times 10^{-12}$ esu leading to $\langle\gamma\rangle = 0.125 \times 10^{-30}$ esu. The second hyperpolarizability of H_2TTP shows an order of magnitude enhancement over H_2TPP obtained from 532 nm picosecond DFWM experiments.

The resonant (422 nm) *B*-band third-order susceptibility from electroabsorption measurement (from Figure 4) obtained as $\chi^{(3)} = 282.7 \times 10^{-12}$ esu, shows an order of magnitude higher than the value at 595 nm, $\chi^{(3)} = 16.7 \times 10^{-12}$ esu. One of the reasons as to why the enhancement of nonlinear susceptibility corresponding to the *B*-band is not more than an order of magnitude could be due to resonance absorption of one of the *Q*-bands whose peak lies around 595 nm. DFWM experiment performed with 532 nm pumped 595 nm dye laser yields the value of the third-order nonlinearity at 595 nm to be $\chi^{(3)} = 9.14 \times 10^{-12}$ esu.

The nonlinear susceptibilities obtained through FWM experiments depend on nonlinear absorption processes such as excited state absorption (two photon or multi-photon processes) and the values for the third-order nonlinearity are extracted using a suitable model[20] of the electronic structure of the porphyrin. However, the values obtained from electroabsorption experiment are directly from the recorded spectrum and is calculated under the single photon transition itself. The nonlinear susceptibilities have been calculated based on the assumption that the electroabsorption spectrum follows the first-order derivative of the absorption spectrum, as discussed by Liptay[23].

Conclusion

Electroabsorption studies have been performed on H_2TTP to probe its third-order optical nonlinearity. The 2Ω spectrum resembles the simple first derivative of the unperturbed absorption spectrum of the porphyrin sample, indicating that the contribution to the stark spectrum arises purely from changes in polarizability. The effective second hyperpolarizability of the porphyrin–polymer system at 532 nm is estimated to be 0.388×10^{-30} esu, which compares well with picosecond DFWM second hyperpolarizability. Electroabsorption thus becomes a useful and cost-effective tool to measure third-order nonlinear susceptibility. However, if one can successfully record the stark spectrum at the higher order harmonics of the applied electric field, one can deduce higher order nonlinearities by deriving equations similar to eqs (5) and (6) for $\chi^{(5)}$ and $\chi^{(7)}$ as well. Thus stark spectroscopy can be exploited to extract higher order nonlinearities, provided the electroabsorption line shape enables Liptay-type analysis.

1. Stark, J., *Ann. Phys.*, 1914, **43**, 965–982.
2. Schulman, R. G. and Townes, C. H., *Phys. Rev.*, 1950, **77**, 500–506.
3. Liptay, W., *Angew. Chem., Int. Ed. Engl.*, 1969, **8**, 177–188.
4. Labhart, H., *Adv. Chem. Phys.*, 1967, **13**, 179–204.
5. Czekalla, *Chimia*, 1961, **15**, 26–31.
6. Mathies, R. and Stryer, L., *Proc. Natl. Acad. Sci. USA*, 1976, **73**, 2169–2173.
7. Handler, P. and Aspnes, D. E., *J. Phys. Chem.*, 1967, **47**, 473–475.
8. Park, E. S. and Boxer, S. G., *J. Phys. Chem. B*, 2002, **106**, 5800–5806.
9. Bublitz, G. U. and Boxer, S. G., *Annu. Rev. Phys. Chem.*, 1997, **48**, 213–242.
10. Weiser, G. and Horvath, A., *Chem. Phys.*, 1998, **227**, 153–166.
11. Vance, F. W., Williams, R. D. and Hupp, J. T., *Int. Rev. Phys. Chem.*, 1998, **17**, 307–329.
12. Wagner, R. and Lindsey, J. S., *J. Am. Chem. Soc.*, 1994, **116**, 9759–9760.
13. Jun-Hong Chou, Kosal, M. E., Nalwa, H. S., Rakow, N. A. and Suslick, K. S., In *The Porphyrin Handbook* (eds Kadish, K., Smith, K. and Guilard, R.), Academic Press, New York, 2000, vol. 6, pp. 13, 14; 29–35.
14. Prem Kiran, P., Raghunath Reddy, D., Maiya, B. G., Dharmadhikari, A. K., Ravindra Kumar, G. and Desai, N. R., *Appl. Opt.*, 2002, **41**, 7631–7636.
15. Anderson, H. L. *et al.*, *J. Mater. Chem.*, 2001, **11**, 312–320.
16. Boyd, R. W., *Nonlinear Optics*, Academic Press, London, 1992.
17. Nobuhiro Ohta, Yuji Iwaki, Takashi Ito, Iwao Yamazaki and Atsuhiro Osuka, *J. Phys. Chem. B*, 1999, **103**, 11242–11245.
18. Stern F., *Phys. Rev.*, 1964, **133**, A1653–A1664.
19. Houlin Zhou and Boxer, S. G., *J. Chem. Phys. B*, 1998, **102**, 9139–9147.
20. Rao, S. V., Studies of excited state dynamics, third order optical nonlinearity and nonlinear absorption in C60, porphyrins and phthalocyanines using incoherent laser spectroscopy, Ph D thesis, University of Hyderabad, 2000.
21. Rao, S. V., Srinivas, N. K. M. N., Rao, D. N., Giribabu, L., Maiya, B. G., Philip, R. and Kumar, R., *Opt. Commun.*, 2000, **182**, 255–264.
22. Maloney, C., Byrne, H., Dennis, W. H., Blau, W. and Kelly, J. M., *Chem. Phys.*, 1988, **121**, 21–39.
23. Liptay, W., Dipole moments and polarizabilities of molecules in excited electronic states. In *Excited States* (ed. Lim, E. C.), Academic Press, New York, 1974, pp. 129–229.

ACKNOWLEDGEMENT. Financial assistance for this work from the Department of Science and Technology is acknowledged.

Received 25 November 2003; revised accepted 1 April 2004